Defence Science Journal, Vol. 75, No. 4, July 2025, pp. 512-519, DOI : 10.14429/dsj.19832

Numerical Optimization of a Radial Inflow Turbine Based on a Loss Model of a Cryogenic Turboexpander Using the Slime Mould Algorithm

Anumay Kumar* and Amrik Singh

Department of Mechanical Engineering, Sant Longowal Institute of Engineering and Technology, Longowal - 148 106, India

**E-mail: anumay_pme1907@sliet.ac.in*

ABSTRACT

The major component of the cryogenic turboexpander is the radial inflow turbine; thus, improvements in its design and performance are effective for the system. The inspirations of six design parameters, including velocity ratio, inlet and outlet impeller diameters, mass flow rate, and blade height, are examined in the context of the total-to-static efficiency of the RIT turbine cryogenic turboexpander. A 1-D design of the radial-inflow turbine has been implemented through MATLAB 2020. In this paper, A novel artificial intelligence system slime mould algorithm (SMA) was employed for the numerical optimization of RIT through MATLAB 2020. An innovative MATLAB script was created for this optimization. The parameters of mass flow rate, number of blades, and blade angles were varied in a constrained range for optimization. This paper explores five distinct blade scenarios for design and numerical optimization processes through MATLAB 2020. The optimization of radial inflow turbines will require the development of a greater capacity of the cryogenic liquefaction system. The performance measurement of the radial inflow turbine was done based on total-to-static efficiency. In numerical optimization, the selection of blades in the range of 11–15 resulted in an improvement in the total-to-static efficiency by around 1.46 %, specifically for 13 blades. This enhancement represents a significant 5.0 % improvement over the results presented in the ANN model explored in the available literature. The maximum total-to-static efficiency achieved through SMA optimization is 89.94 % for 15 blades.

Keywords: Slime mould algorithm; MATLAB; Radial inflow turbine; Total-to-static efficiency

NOMENCLATURE

t	: Blade thickness
p	: Pressure (pa)
b	: Blade height(mm)
R_h	: Hub radius (mm)
U	: Blade speed (m/s)
α	: Absolute velocity angle
W	: Relative velocity(m/s)
v_s	: Velocity ratio
c	: Turbine blade chord
Z	: Number of blades
ORC	: Organic Rankine cycle
Z_r	: Rotor axial length(m)
h	: Enthalpy (KJ/kg)
D_h	: Mean passage hydraulic diameter
SMA	: Slime mould algorithm
1	: Turbine inlet
L_h	: Mean pressure hydraulic length
2	: Turbine outlet
CFD	: Computational fluid dynamics
r_3	: Turbine outlet radius(mm)
M	: Mach number
R_s	: Shroud radius(mm)
ANN	: Artificial neural network
R_p	: Pressure ratio
ANFIS	: Adaptive neuro-fuzzy inference system
β_2	: Inlet blade angle
RIT	: Radial inflow turbine
β_3	: Outlet blade angle
r_2	: Turbine inlet radius(mm)
m	: Mass flow rate (kg/s)

Received : 23 January 2024, Revised : 11 February 2025
Accepted : 15 March 2025, Online published : 26 June 2025

1. INTRODUCTION

The purpose of this work is to enhance the total-to-static efficiency and performance of a cryogenic turboexpander, which can be used for liquefaction and refrigeration systems. This holds significance for a range of uses, including creating an inert welding environment (using shielding gas), leak detection, optical fibres, solar telescopes, superconductors, and various biomedical and chemical instruments[1]. Radial inflow turbines have been applied in diverse engineering sectors, including power generation systems, liquefaction and refrigeration plants, superconductors, and nuclear fusion applications[2]. Cryogenic turboexpander-based gas liquefaction processes are particularly vital for industrial and research purposes. The radial inflow turbine serves as the primary component for this type of refrigeration, and the liquefaction cycle has numerous other uses, such as in gas turbines, the organic Rankine cycle (ORC), and air separation[3]. The process involved conducting multi-goal optimization for the ORC, the radial inflow turbine was analysed using ANSYS CFX and design exploration based on a 3D Reynolds-average Naiver-Stokes (RANS) and a k-omega SST turbulence model. For the optimization of blade geometry, 20 design points were considered, with blade angles and thickness distribution being represented using the B-splines technique. Isopentane and R245fa have been used as organic working fluids.

The increment of thermal efficiency for both cycles is around 13.95 % and 17.38 %[4]. High-pressure ratio radial inflow turbines are predominantly employed in organic Rankine cycle power systems. These turbines have been subjected to multi-goal optimization using a genetic algorithm for various high-pressure ratio applications. The resulting model predicts isentropic efficiency within a margin of ±3 %.[5] The thermodynamic properties and performance of turbo-expanders have been enhanced by directly incorporating the Hepak database for real gas properties into the computational fluid dynamics (CFD) solver[6]. In the case of small-scale turbines, a non-dimensional performance map shows a significant impact on the shroud-to-tip radius ratio[7]. The use of a helium cryogenic system is common in superconducting systems as well as in the fields of nuclear fusion engineering and space exploration. Therefore, there is a critical need to develop a high-efficiency helium turbine featuring splitter blades capable of liquefying 40 litres of helium per hour via the Claude cycle. This can be achieved by learning the thermodynamic characteristics using an in-house code that can be integrated into the NIST REFPROP database[8].

The slime mould algorithm (SMA) primarily draws inspiration from the natural swinging behaviour of slime mould. The SMA incorporates innovative elements, including a distinctive mathematical model that employs adaptive weights. This model imitates the way slime mould generates positive and negative feedback in its propagation waves, resembling a bio-oscillator. The goal is to show the best path that links food sources while demonstrating exceptional exploratory capabilities and exploitation tendencies[9]. A computational iterative loop compiled by MATLAB has been put into practice to assess the performance of the off-design turbo-expander. The correlation of losses has been integrated into the quantitative picture of flow expansion through the duct. Performance is estimated with the help of total-to-static efficiency, in which the rotational speed is kept in the range of 52,000 to 60,000 rpm[10]. One-dimensional modelling has been used to examine the parameters of the nozzle and turbine. Utilizing artificial intelligence techniques, essential non-dimensional variables like blade speed, pressure ratio, and the ratio between the hub and shroud radii to the turbine inlet radius have been calculated to enhance the turbine's performance.

As a result, turbine efficiency and power output have seen notable improvements, with a 4 % increase in efficiency and an 18.9 % boost in power output in contrast to the existing model. The analysis of fluid flow encompasses various aspects, including the recognition of flow separation zones, tip leakage flows, and the development of vortices at distinct locations along the turbine's span. Sensitivity analysis using the Sobel method has been applied to pinpoint significant parameters. In conclusion, the numerical results have been subjected to comparison to experimental results for validation[11]. In their study, Ghorbanian and Gholamrezaei[12] investigated the act of a compressor using various artificial neural network (ANN) techniques, including GRNN, RGRNN, RBFN, and MLP. They conducted an experimental analysis to assess the temperature drop, isentropic efficiency, and power output of a turboexpander. Their analysis was based on a range of mass flow rates from 0.03 to 0.08 kg/s and inlet temperatures of 130, 140, and 150 K. Notably, the most significant temperature decrease was noted at the inlet temperature of 150 K. The present analysis was also based on a range of mass flow rates from 0.03 to 0.08 kg/s and inlet temperatures of 130, 140, and 150 K[13]. MATLAB code was employed to create a first design for a 590-kW radial inflow turbine intended for use in an organic Rankine cycle (ORC) with the organic working fluid R134a.

Furthermore, NIST REFPROP was used to determine the fluid's physical properties. The design process involved the use of seven design parameters, and the particle swarm optimization algorithm was applied to maximize the overall total-to-static efficiency[14]. The supercritical carbon dioxide (SCO_2) power cycle has a critical component radial inflow turbine[16]. 1-D mean line design and aerodynamic design and analysis of a radial inflow turbine for supercritical CO_2 mixtures. Rotational speed limits the design of the radial inflow turbine and total-to-static efficiency. Clearance-to-blade height ratio, pressure ratio, and fluid viscosity defences in the turbine efficiency. The aerodynamics of all working fluids behaved similarly. The aerodynamic performance was improved by doping CO_2. The working fluid is the deciding factor for the size of the rotor and velocity and mechanical components like the type of bearing[18]. Hydrogen can be stored in a gaseous state at high pressure and in a liquid state at cryogenic temperature.

A liquid hydrogen tank needs insulation to prevent heat leakage. Pressure behaviour and internal pressure conditions

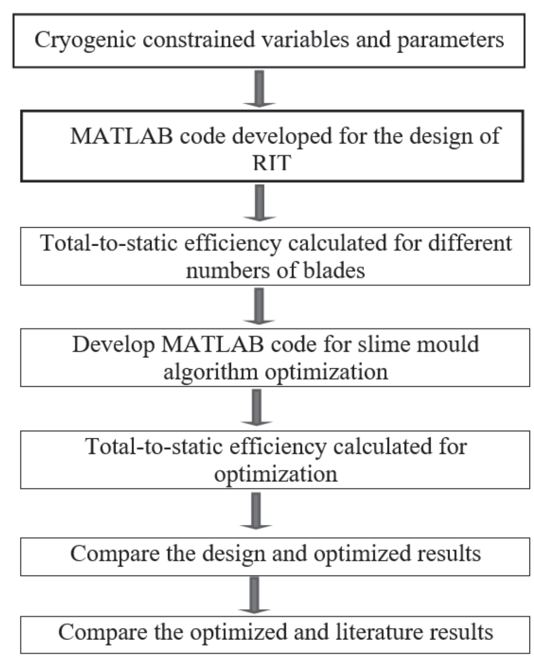

Figure 1. Flow chart of the methodology.

have been monitored by the thermodynamic model of the cryogenic liquid hydrogen tank. Transient analysis has been performed for fuel consumption rate. There is a time delay between the charging and consumption of fuel by the tank, which deliberately affects the fuel tank[19].

2. RADIAL INFLOW MEAN-LINE DESIGN METHOD

Figure 1 shows the methodology of the design and the optimization of the radial inflow turbine for the cryogenic turboexpander.

2.1 Design Method

The first and most crucial step in cryogenic turboexpander design is the 1-D design. The given inlet of the radial turbine can predict the geometrical design. The description of the turbine is contingent upon the working fluid. The intention is to decrease the temperature per cryogenic concern. Obtaining this condition requires the inlet and outlet radii to be diverse. In this paper, a radial turbine has been modelled for the cryogenic turboexpander. The inlet situations of the turbine have been chosen for training. The inlet temperature is 122 K. The inlet pressure is about 6 bar, and the discharge pressure is 1.5 bar. The stream rate chosen in consideration of turbine geometry is 0.03–0.08 kg/s.

2.2 Empirical Loss Model

The one-dimensional strategy of a radial inflow turbine demands significant effort and resources. The radial inflow turbine's dimensions depend on the specific fluid used in the cryogenic turboexpander. When designing a radial inflow turbine for a cryogenic turboexpander, it is essential to account for the challenges associated with cryogenic conditions. Several factors, such as incidence loss, tip clearance loss, and friction loss, have a noteworthy impact on the efficiency calculations[11]. The study includes the construction of different loss components, which are listed below. The nomenclature and symbols for the variables are provided in Table 1.

The steps involved in the 1-D design of RIT are as follows: The first step involves estimating a first worth for the total-to-static efficiency, which plays a crucial role in figuring out the spouting velocity.

Assume η_{ts}=85 %

$$\Delta H_{ideal} = \frac{H_{02} - H_{03}}{\eta_{ts}} \tag{1}$$

$$H_{02} - H_{03} = \frac{28940J}{kgK}$$

This value is taken from a prototype turbine of Subrata Kumar Ghosh's thesis.

$$\Delta H_{ideal} = \frac{28940}{0.85} = 34047.05$$

$$c_{os} = \sqrt{2}\ \Delta H_{ideal} \tag{2}$$

Here, ΔH_{ideal} stands for the ideal total-to-static enthalpy decrease, H_0 signifies the total enthalpy, ηts denotes the total-to-static efficiency, and c_{os} stands for the spouting velocity. The first blade speed at the inlet is found and grounded on the velocity ratio, which is then used to estimate the absolute rotor velocity.

$$U_2 = v_s \cdot c_{os} \tag{3}$$

2.2.1 Incidence Loss (Δh_t)

In line with this loss mechanism, there is a transformation of kinetic energy into the internal energy of the fluid. This occurrence has been articulated as follows:

$$\Delta h_t = \left[\frac{W_2^2 \cos\ \beta - \beta_{2,opt})}{2} \right] \tag{4}$$

Here, $\beta_{2,opt}$ stands for the incidence angle, which is defined as follows:

$$\cot \beta_{2,opt} = \frac{-1.98 \cot(\alpha_2)}{z\left(1 - \frac{1.98}{z}\right)} \tag{5}$$

2.2.2. Passage loss ($\Delta h_{passage}$)

The mean kinetic energy factor addresses the loss experienced during passage. It has been mathematically defined as follows

$$\Delta h_{passage} = k_p \left\{ \left(\frac{L_h}{D_h}\right) + 0.68\left[1 - \frac{r_t}{r_2}\right] * \frac{\sin\beta_3}{\frac{b_{3m}}{c}} \right\} * \left[\left(\frac{W_2^2 + W_3^2}{2}\right)\right] \tag{6}$$

k_p = 0.2.L_h, D_h, and c are commonly known as the mean hydraulic length of the passage, the passage diameter, and the length of the chord for the turbine blade, respectively.

2.2.3. Rotor Clearance Loss Δh_{cl}

The turbine clearance loss is influenced by both the axial (Ɛx) and radial (Ɛr) clearances within the turbine, and it has been mathematically expressed as follows:

$$\Delta h_{cl} = \frac{U_2 z}{8\pi}\left(k_x \varepsilon_x C_x + k_r \varepsilon_r C_r + k_{xr}\sqrt{\varepsilon_x C_x \varepsilon_r C_r}\right) \tag{7}$$

$$C_x = \left(\frac{1 - r_{3sh}}{Cm_2 * b_2}\right) \tag{8}$$

$$C_r = \left(\frac{r_{3sh}}{4} * \left(\frac{(Z_r - b_2)}{Cm_3 * r_3 * b_3}\right)\right) \tag{9}$$

In this context, k_x stands for the discharge coefficient in the axial direction, k_r stands for the discharge coefficient in the radial direction, and k_{xr} is the coefficient that accounts for cross-coupling effects. These constants have been assigned values of 0.40, 0.75, and -0.3, respectively.

2.2.4 Trailing Edge Loss Δh_{TEL}

When modelling trailing edge loss, we assume that the relative pressure drop at the turbine's exit varies in direct proportion to the relative kinetic energy.

$$\Delta p_{rel} = P_{3rel} - p_{2rel} = \frac{\rho_3 W_3^2}{2}\left[\frac{Zt}{\pi r_t \cos\beta_3}\right] \tag{10}$$

The process involves converting the pressure loss formulation into a loss coefficient.

$$\Delta h_{TEL} = \frac{2}{\gamma M_{3rel}^2} * \frac{\Delta p_{rel}}{p_{3rel}} \tag{11}$$

2.2.5 *Blade Loading Loss Δh_{BL}*

Boundary layer separation stands for a secondary loss that contributes to blade loading loss. This loss occurs because of the curvature in the blade profile, and it has been expressed as follows:

$$\Delta h_{BL} = 2\frac{\left(W_2 - U_2\right)^2}{\frac{ZL}{r_2}} \tag{12}$$

The total loss was formulated as:

$$\sum h_{Lt} = \Delta h_l + \Delta h_{passage} + \Delta h_{cl} + \Delta h_{TEL} + \Delta h_{BL} \tag{13}$$

$$\eta_{ts} = \frac{h_0}{h_0 + \sum h_{Lt}} \tag{14}$$

The total-to-static efficiency will be changed by incorporating distinct types of losses [6]. The value of h_0 is 28,940 J/kg.

2.2.6 *Blade Inlet Angle*

The calculation of the circumferential velocity component at the turbine's inlet can be performed as follows:

$$C_{\theta 2} = \frac{2K}{d_2} \tag{15}$$

$$K = K_1 Q \tag{16}$$

In the case of critical flow conditions, K_1 stands for a constant and Q denotes the mass flow rate.

$$Q_c = \frac{n\pi d_2^2}{120 k_1} \tag{17}$$

With d_2 being 24.90 mm, rotational speed equalling 140,000 rpm, and Q_c measuring 0.1 kg/s, the value of k_1 has been determined to be 22.724. Consequently, we obtain the Eqn. $C_{\theta 2}$= 1824.337, multiplied by the mass flow rate, based on the velocity triangle.

$$C_{m2} = \frac{\left(U_2 - C_{\theta 2}\right)}{\tan \alpha_2} \tag{18}$$

By adjusting the mass flow rate for various Cm_2 values, we can calculate the relative velocity at the turbine's inlet as follows:

$$W_2 = \frac{C_{m2}}{\cos \beta_2} \tag{19}$$

2.2.7 *Blade Outlet Angle β_3*

The outlet flow angle is taken to vary in response to changes in the mass flow rate, with six distinct values being examined for the outlet flow angle. We can calculate the meridian velocity at the outlet using the following formula:

$$C_{m3} = \frac{Q_r}{A_3} \tag{20}$$

Considering A_3 as the outlet cross-sectional area, we've calculated that Q_r is 0.00397 m^3/s and d_3 is 15.60 mm. Balaji has recommended a C_{m3} value of approximately 20 m/s. Consequently, we have determined the relative velocity at the turbine's exit using the velocity triangle as follows:

$$W_3 = \frac{C_{m3}}{\cos \beta_3} \tag{21}$$

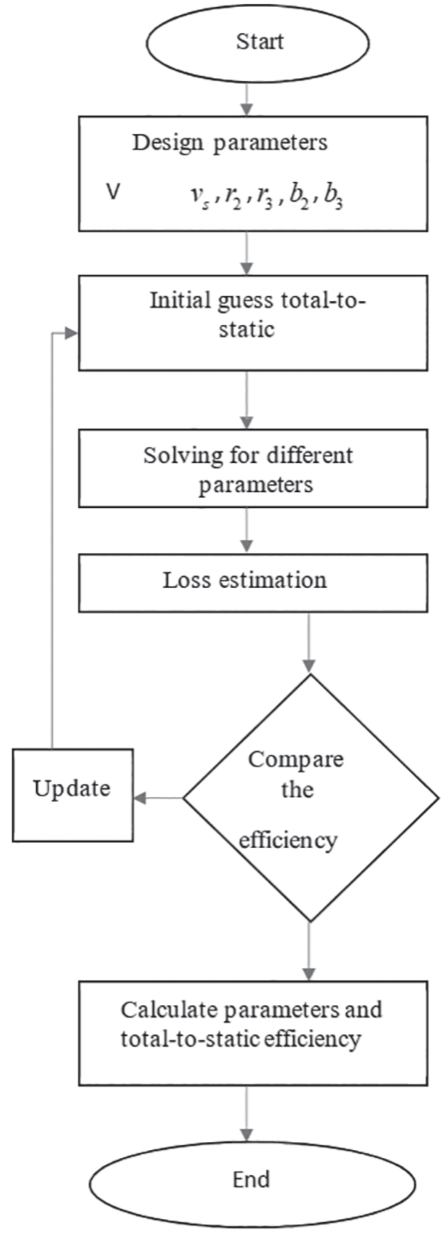

Figure 2. Flow chart for the best preliminary design with the SMA.

2.3 Approach for Optimizing the Initial Design

The universal principle of the best first strategy of radial turbines is portrayed in the flowchart in Fig. 2. The 1-D design of a radial inflow turbine involves distinct sets of parameters. Total-to-static efficiency depends on nine different parameters: $\eta_{ts} = f(\beta_2, \beta_3\ r_2, r_3, b_2, b_3$, mass flow rate, α_2, vs). These nine parameters have stimulated the total-to-static effectiveness. In the present investigation, we computed the total-to-static efficiency using a loss model as the basis. The loss model depends on the range of nine design parameters. The range of radial-inflow turbine design parameters is shown in Table 1[15]. The design results from distinctive design variables are constrained to the range.

Table 1. Constrained tange cryogenic application

Design variables	Range
Inlet stagnation pressure (bar)	8–10
Inlet stagnation temperature (K)	90–180
Mass flow rate (kg/s)	0.01–0.09
Blade speed ratio	0.62–0.82
Blade inlet angle (degrees)	72–82
Number of blades (Z)	10–15
Pressure ratio	2–5
Rotational speed (RPM)	80,000–150,000

2.3.1 SMA

Hereafter, the slime mould algorithm is chosen to achieve design optimization to increase total-to-static efficiency. The slime mould algorithm is primarily inspired by the natural oscillation behaviour shown by slime mould. The mathematical equation of slime mould follows the rule below to emulate the contraction mode:

$$X_{t+1} = \left\{ X_b(t) + v_b\left(W * X_A(t) - \mathrm{X}_B(t)\right)\right\} r \angle p \qquad (22)$$

In the above equation, v_b is a parameter which varies in the array of [-a, a], and vc declines since 1 to 0. The iteration is represented by 't'. The position of the slime mould is denoted as 'X', and the randomly selected forms within the swarm are 'X_A' and 'X_B', with 'W' standing for the weight of the slime mould. The highly concentrated location is X_b, and p can be represented by

$$p = \tanh\left|S(i) - \mathrm{DF}\right| \qquad (23)$$

The fitness of 'X' can be represented as 'S(i)', and the best fitness across all iterations can be written as 'DF, i ϵ 1, 2, ……, n.

The formula for v_b is

$$v_b = \left[-alpha, alpha\right] \qquad (24)$$

where

$$alpha = \operatorname{arctan} h\left(-\left(\frac{iter}{\max iter}\right) + 1\right) \qquad (25)$$

W can be represented by

$$W\left(SmellIndex(i)\right) = \begin{cases} \left\{ 1 + r\log\left(\dfrac{b_F - \mathrm{S}(i)}{b_F - w_F} + 1\right) Condition \right. \\ \left. 1 - r\log\left(\dfrac{b_F - S(i)}{b_F - w_F} + 1\right) Others \right\} \end{cases} \qquad (26)$$

$$SmellIndex = sort(S) \qquad (27)$$

In the above, the state appoints S(i)' corresponds to the first half of the population., r lies between [0,1], 'b_F' stands for the best fitness in the current iteration, and 'w_F' stands for the poorest fitness values in the current iterative loop. 'Smell Index' stands for a sequence of sorted fitness values.

The mathematical modelling process has been employed to update the slime mould's position, which can be expressed as follows:

$$X^* = \begin{cases} rand\left(UB - \mathrm{LB}\right) + \mathrm{LB\ rand} < \mathrm{Z} \\ X_b(t) + v_b\left(WX_A(t) - X_B(t)\right) r < p \\ v_c X(t) r \geq p \end{cases} \qquad (28)$$

The search scale's lower and upper boundaries are defined as LB and UB, respectively, with 'rand' and 'r' representing random values within the range [0,1]. The iteration further increases, and the rate of v_b oscillates arbitrarily [-alpha, alpha] and slants toward 0. The slime mould algorithm equation has been obtained from[17], and the paper introduces a novel approach to stochastic optimization.

3. RESULTS AND DISCUSSION

The 1-D design of the radial inflow turbine used for a cryogenic turboexpander application was performed through MATLAB original code, and then the slime mould algorithm was performed through MATLAB original code. The total-to-static efficiency for radial inflow turbine has improved in 1-D design and optimization simulation. The design variables for radial turbine constrained in a cryogenic application are shown in Table 2. Total-to-static efficiency increased from 83.86 % to 86.21 % for the velocity ratio of 0.62, as the α_2 varied from 72 to 82 degrees. There was an increase in total-to-static efficiency of 2.35 % by the variation in the absolute flow angle by 72 to 82 degrees. For the number of blades (Z=13), when the mass flow rate increased from 0.03 to 0.08, the total-to-static efficiency increased from 87.11 % to 87.31 %.

3.1 1-D Design Result

MATLAB code was developed for the 1-D design of a radial inflow turbine per cryogenic constraints.

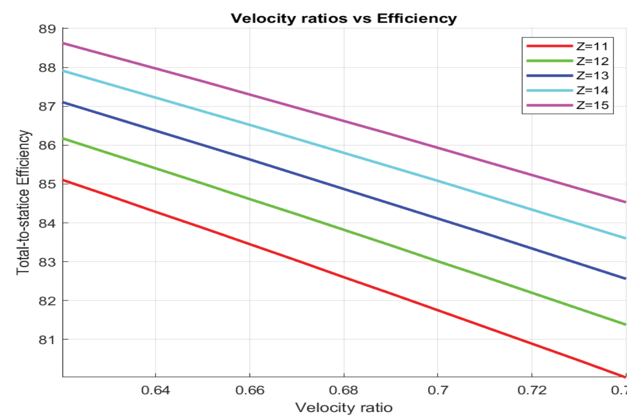

Figure 3. Velocity ratios vs efficiency for different numbers of blades.

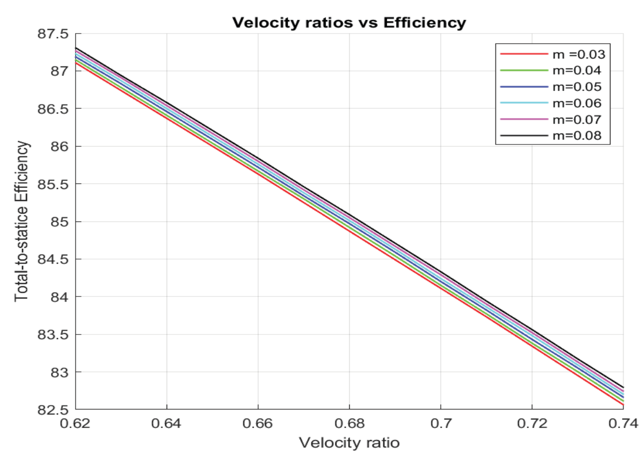

Figure 4. Velocity ratio varies with efficiency for different mass flow rates.

The 1-D design results obtained through MATLAB original code are represented in Fig. 3. Velocity ratios vary with the total-to-static efficiency for different numbers of blades. As velocity ratios increase, total-to-static efficiency decreases. The maximum efficiency was reached at a velocity ratio of 0.62.

Figure 4 demonstrates the result for Z = 13. The mass flow rate changed from 0.03 to 0.08 kg/s. As the mass flow rate increased from 0.03 to 0.04, the efficiency rose from 87.11 to 87.15 %. The total-to-static efficiency increased from 0.04 % as the mass flow rate grew.

Table 2. 1-D design and optimized design for varying blade quantities

Number of blades	1-D design total-to-static efficiency	Numerical optimized total-to-static efficiency	Improvement in total-to-static efficiency
11	85.11	86.76	1.65
12	86.18	87.73	1.55
13	87.11	88.57	1.46
14	87.92	89.30	1.38
15	88.63	89.94	1.31

Table 3. SMA optimized result vs ANN result

Design output parameter	Optimized model	Kumar, *et al.* (ANN result)	Difference
Blade height Turbine inlet b_2 (mm)	2.0	2.14	0.14
Blade height Turbine outlet b_3 (mm)	1.00	1.01	0.01
Turbine outlet diameter d_3 (mm)	15.8	15.71	0.09
Turbine inlet diameter d_2 (mm)	25.2	25.64	0.44
Outlet blade angle (β3) (degrees)	-79.5	-84.76	-5.26
Inlet blade angle (β2) (degrees)	-51.5	-55.12	-3.62
Blade speed (U_2) (m/s)	159.309	144.62	14.689
Total-to-static efficiency	88.57	83.57	5

3.2 Numerical Optimization Results

SMA optimization was conducted under distinctive design variables in a constrained range of cryogenic applications. The optimization process was designed to maximize the total-to-static efficiency. The number of population NP = 100, and the number of dimensions was kept at D = 9. The slime mould algorithm was initialized by creating a population of 100 slime moulds with a nine-dimensional structure. The SMA constraints were V_b and Vc. The number of iterations runs for this algorithm was 100, and the fitness function was the total-to-static efficiency. Finally, parameters were obtained for the radial-inflow turbine geometries for maximum total-to-static efficiency. Table 2 displays the outcomes of both the mean-line design and the optimization design using the SMA for the radial inflow turbine employed in the cryogenic turboexpander. For verification purposes, the obtained radial turbine model was compared with the existing model of M. Kumar et al. (see Table 3). The ANN-optimized result was also compared with an existing SMA-optimized model. A 5 % increase in total-to-static efficiency has been identified.

The enhancement in total-to-static efficiency is 1.65 % for 11 blades, 1.55 % for 12 blades, 1.46 % for 13 blades, 1.38 % for 14 blades, and 1.31 % for 15 blades.

3.3 Impact Analysis of Design Parameters

The parameters used in the strategy of the radial inflow turbine influenced the total-to-static efficiency. Total-to-static efficiency varied with these design variables as revealed in Fig. 5 and Fig. 6.

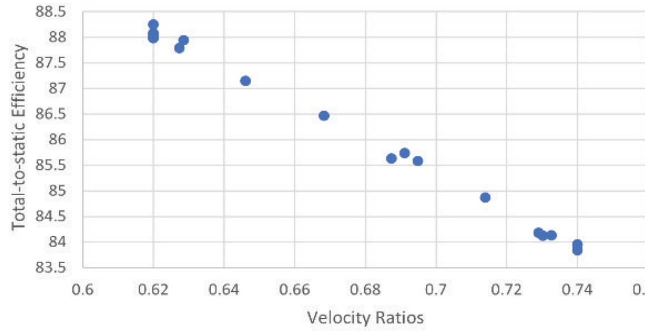

Figure 5. Efficiency in relation to the velocity ratio.

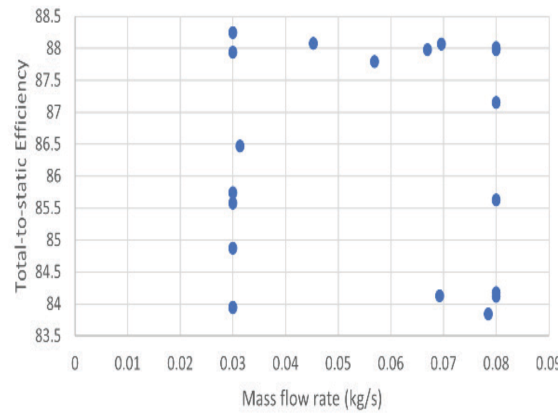

Figure 6. Total-to-static efficiency vs mass flow rate.

Figure 5 displays a graph of velocity ratios vs total-to-static efficiency in which efficiency is perfected as the velocity ratios vary. However, as revealed in the figure, the velocity ratio converges to 0.62. The highest total-to-static efficiency was reached at a velocity ratio of 0.62. There is a decreasing trend as the velocity ratio rises, resulting in a reduction in total-to-static efficiency.

Figure 6 shows the variation of mass flow rate with total-to-static efficiency. According to the results from the optimization simulation, the highest efficiency is reached when the mass flow rate is 0.03 kg/s. In the 1-D design of the radial turbine, maximum efficiency was achieved at 0.08 kg/s. Thus, the mass flow rate decreases until it reaches 0.055 kg/s and then begins to rise once more. The optimized design for a radial turbine intended for cryogenic applications achieved its highest total-to-static efficiency at a blade inlet angle of 72°. As the blade inlet angle increased, the total-to-static efficiency was reduced, particularly at 82°, which resulted in the lowest total-to-static efficiency.

4. CONCLUSION

In the present research, a mean-line design and multi-variable optimization process were created for a radial inflow turbine used in a cryogenic turboexpander. This development can be verified by a comparison with earlier literature. The slime mould algorithm was used to conduct a comprehensive design and global optimization process. This algorithm achieved the highest total-to-static efficiency. The distinctive design parameters were perfected, and their impact on the total-to-static efficiency of the radial-inflow turbine was analysed. The working fluid was liquid nitrogen, and the main conclusion is as follows. The application of the slime mould algorithm led to a 1.46 % enhancement in total-to-static efficiency. The ANN results presented by M. Kumar, *et al.* showed an efficiency of 83.6 %. The increase in total-to-static efficiency was approximately 5.0 %.

Five different cases were studied according to the number of blades in the cryogenic application-constrained range. Improvements in the efficiency of these five cases were significant, at 1.65 % for 11 blades, 1.55 % for 12 blades, 1.38 % for 14 blades, and 1.31 % for 15 blades. Blade speed varied with velocity ratios such that rotational speed is considered but as per Cryogenic constrained conditions. The number of blades can be optimized by computational fluid dynamics (CFD), but such an analysis was not considered in this manuscript.

The velocity ratio of 0.62 resulted in the maximum total-to-static efficiency. Mass flow rates and blade inlet angles are about 0.03 kg/s and 72°.

5. FUTURE SCOPE

An optimized radial inflow turbine of a cryogenic turboexpander can be used for the liquefaction of hydrogen. The optimized design of a radial inflow turbine can be used for supercritical CO_2 mixtures.

REFERENCES

1. Kumar M, Behera SK, Kumar A, Sahoo RK. Rotational effect on flow field and thermal characteristics of a turboexpander for helium liquefaction system: a numerical perspective. Journal of Heat Transfer. 2020 Nov 1;142(11):112901.
doi:10.1115/1.4047838
2. Ghorbanian K, Gholamrezaei M. An artificial neural network approach to compressor performance prediction. Applied Energy. 2009 Jul 1;86(7-8):1210-21.
doi: 10.1016/j.apenergy.2008.06.006
3. Kumar M, Biswal R, Behera SK, Sahoo RK, Pal S. Experimental and numerical approach for characterization and performance evaluation of cryogenic turboexpander under rotating condition. International Communications in Heat and Mass Transfer. 2022 Jul 1;136:106185.
doi: 10.1016/j.icheatmasstransfer.20 22.106185
4. Al Jubori AM, Al-Dadah R, Mahmoud S. Performance enhancement of a small-scale organic Rankine cycle radial-inflow turbine through multi-objective optimization algorithm. Energy. 2017 Jul 15; 131:297-311.
doi: 10.1016/j.energy.2017.05.022
5. Maroni A, Robertson M, Martinez-Botas R, Haglind F. A methodology for the preliminary design and performance prediction of high-pressure ratio radial-inflow turbines. Energy. 2018 Dec 1; 164:1062-78
doi: 10.1016/j.energy.2018.09.045
6. Ke C, Xiong L, Peng N, Dong B, Li K, Li J, Liu L. Performance analysis of high-speed cryogenic turbo-expander at cooling process based on numerical and experimental study. International Journal of Refrigeration. 2021 Feb 1; 122:81-96
doi: 10.1016/j.ijrefrig.2020.09.0 16
7. Mounier V, Olmedo LE, Schiffmann J. Small scale radial inflow turbine performance and pre-design maps for Organic Rankine Cycles. Energy. 2018 Jan 15; 143:1072-84.
doi: 10.1016/j.energy.2017.11.002
8. Li X, Lv C, Yang S, Li J, Deng B, Li Q. Preliminary design and performance analysis of a radial inflow turbine for a large-scale helium cryogenic system. Energy. 2019 Jan 15; 167:106-16.
doi: 10.1016/j.energy.2018.10.179
9. Li S, Chen H, Wang M, Heidari AA, Mirjalili S. Slime mould algorithm: A new method for stochastic optimization. Future Generation Computer Systems. 2020 Oct 1;111: 300-23.
doi: 10.1016/j.future.2020.03.055
10. Niu L, Meng Y, Chen S, Li X, Zeng Q, Lou F, Hou Y. Off-design performance analysis of cryogenic turbo-expander based on mathematic prediction and experiment research. Applied Thermal Engineering.2018 Jun 25;138:873-87.
doi: 10.1016/j.applthermaleng.2018 .02.024
11. Kumar M, Behera SK, Kumar A, Sahoo RK. Numerical and experimental investigation to visualize the fluid flow and thermal characteristics of a cryogenic turboexpander. Energy. 2019 Dec 15;189:116267.
doi:10.1016/j.energy.2019.116267
12. Ghorbanian K, Gholamrezaei M. An artificial neural network approach to compressor performance prediction. Applied Energy. 2009 Jul 1;86(7-8):1210-21.
doi:10.1016/j.apenergy.2008.0 6.006
13. Kumar M, Panda D, Behera SK, Sahoo RK. Experimental investigation and performance prediction of a cryogenic turboexpander using artificial intelligence techniques. Applied thermal engineering.2019 Nov 5;162:114273.
doi:10.1016/j.applthermaleng.2019 .114273
14. Zhang C, Li Y, Tong Z. Impact analysis and optimization of the preliminary design parameters for an organic Rankine cycle radial inflow turbine. Journal of the Brazilian Society of Mechanical Sciences and Engineering. 2023 Jan;45(1):10.
doi: 10.1007/s40430-022-03932-x
15. Kumar M, Panda D, Kumar A, Sahoo RK, Behera SK. A methodology for the performance prediction: flow field and thermal analysis of a helium turboexpander. Journal of the Brazilian Society of Mechanical Sciences and Engineering. 2019 Nov;41(11):484.
doi: 10.1007/s40430-019-1989-z

16. Uusitalo A, Grönman A. Analysis of radial inflow turbine losses operating with supercritical carbon dioxide. Energies. 2021 Jun 15;14(12): 3561. doi:10.3390/en14123561
17. Li S, Chen H, Wang M, Heidari AA, Mirjalili S. Slime mould algorithm: A new method for stochastic optimization. Future Generation Computer Systems. 2020 Oct 1; 111:300-23. doi: 10.1016/j.future.2020.03.055
18. Aqel O, White M, Sayma A. Loss analysis in radial inflow turbines for supercritical CO2 mixtures. Journal of Turbomachinery. 2024 May 1;146(5). doi:10.1115/1.4064193
19. Choi D, Lee S, Kim S. A thermodynamic model for cryogenic liquid hydrogen fuel tanks. Applied Sciences. 2024 Apr 29;14(9):3786. doi:10.3390/app14093786

CONTRIBUTORS

Mr Anumay Kumar is currently pursuing PhD from the Department of Mechanical Engineering SLIET Longowal, Punjab. His research interest is Cryogenic turboexpander, radial inflow turbine.
In the present Study he has developed the MATLAB code for optimization of radial inflow turbine based on Slime mould algorithm.

Dr Amrik Singh is an Associate Professor in Department of Mechanical Engineering at SLIET Longowal-Punjab (India). He obtained PhD from SLIET (Deemed to be University) Longowal-Punjab India. His areas of research include: Turnkey projects, design & engineering in material handling & mineral beneficiation, hydro mechanical gates, and machinery. His area of expertise include: CIMS, flexible manufacturing systems and manufacturing simulation.
In the present Study he has carefully evaluated the manuscript.